THE USE OF SCANNING TRANSITIOMETRY TO INVESTIGATE THERMODYNAMIC PROPERTIES OF POLYMERIC SYSTEMS OVER EXTENDED *T* AND *p* RANGES

J-P. E. GROLIER[1,4], F. DAN[2], S. BOYER[1], M. ORLOWSKA[3], and S.L. RANDZIO[3]

[1]Laboratory of Thermodynamics of Solutions and Polymers, Blaise Pascal University, Aubière, France
[2]Department of Macromolecular Chemistry, Gh. Asachi Technical University, Iasi, Romania
[3]Institute of Physical Chemistry, Polish Academy of Science, Warsaw, Poland
[4]To whom correspondence should be addressed: j-pierre.grolier@univ-bpclermont.fr

ABSTRACT

Scanning transitiometry is a newly developed technique which allows to scan in the working cell of a very sensitive calorimeter one of the independent variables (*p, V* or *T*) while the other independent variable is kept constant. The change of the dependent variable is recorded simultaneously with the thermal effect associated with the process or the system under investigation. In the case of non-reacting systems which remains in a homogeneous state, both the mechanical and thermal outputs thus obtained give straightforward access to different couples of thermomechanical coefficients: α_p and κ_T, β_V and κ_T, C_p and α_p, C_V and β_V, depending on the pair of selected independent variables. When the system or the material sample goes through a chemical reaction or a phase change, the recorded information yields the corresponding heat and *pVT* characteristics. The working cell may also house an optical fiber probe for spectroscopic *in situ* readings from UV to NIR, as well as injection and stirring devices permitting to investigate reacting systems. The actual operating ranges of scanning transitiometry are respectively 173 K < T < 673 K and 0.1 < *p* < 200 MPa (or 400 MPa). With such equipment bulk properties, transitions as well as reactions (*i.e.* polymerization) can be advantageously studied. Selected examples all dealing with polymeric systems (including biopolymers) are illustrated, namely, measurements of thermomechanical coefficients (thermal expansion, compressibility), characterization of transitions (fusion, crystallization, glass transition, gelatinization) and particle synthesis. All examples show that scanning transitiometry is a versatile technique to fully characterize thermophysical properties as well as thermodynamic behavior of a large variety of systems and materials.

KEY WORDS: scanning transitiometry; polymers; high pressure; high or low temperature; reaction calorimetry.

1. INTRODUCTION

Research in polymer science continues to mushroom, producing a plethora of new elastomers, plastics, adhesives, coatings, and fibers. All of this new information is gradually being codified and unified with important new theories about the interrelationships among polymer structure, physical properties, and useful behavior. Thus the ideas of thermodynamics, kinetics, and polymer chain structure work together to strengthen the field of polymer science [1].

Thermal methods of analysis have always been widely used in investigation of polymer properties, especially in the case of phase transitions. Phase transitions are very important in industrial practice, before all ignorance of a phase diagram, particularly at extreme conditions of pressure, temperature, and of chemical reactivity, is a limiting factor to the development of an industrial process, sol-gel transitions, polymerization under solvent near supercritical conditions, micro- and nanofoaming processes, etc [2].

Calorimetry is a very versatile method to measure thermodynamic properties of substances and to follow phase change phenomena or chemical reactions. In most applications, calorimetry is carried out at constant pressure while the tracked phenomenon is observed on increasing or decreasing the temperature (either stepwise or at constant scanning rate) [3]. Many studies carried out at constant pressure (different from atmospheric pressure) were achieved by some authors [4-6] who investigated the influence of this state variable on the thermodynamic properties. Mostly these investigations were done under isothermal conditions and pressure changes were made step-wise [7,8] or at a constant rate [9,10].

The possibility of controlling the three most important thermodynamic variables (pVT) in calorimetric measurements makes it possible to perform simultaneous measurements of changes or rates of such changes of both thermal and mechanical contributions to the thermodynamic potential change caused by the perturbation [11]. When referring to the Ehrenfest classification of transitions [12] one can easily understand how useful is the simultaneous recording of both mechanical and thermal derivatives in the analysis of transitions and interpretation of their nature, especially in complex systems. The simultaneous determination of both thermal and mechanical contributions to the total change of thermodynamic potential not only leads to the complete thermodynamic description of the system under study, but also permits investigation of systems with limited stability or systems with irreversible transitions. This approach is also very useful in analyzing the course of a transition. By a proper external change of the controlling variable the transition under investigation can be accelerated, impeded or even stopped at any degree of its advancement and then taken back to the beginning, all with simultaneous recording of the heat and mechanical variable variations. This permits not only determination of the total changes of the thermodynamic functions for the transition but also allows analysis of their evolution along the advancement of the transformation. For this reason the technique was called scanning transitiometry [13]. The technique can operate over wide pressure (up to 400 MPa) and temperature (173–673 K) ranges with the step-wise or the linear scan of the variable change. It was already applied in investigation of systems of various nature such liquid-crystals, polymers, dense liquids [14,15]. Scanning transitiometry is particularly useful in determining pressure effects on various phase transitions in polymeric systems [6] and in measuring the thermomechanical coefficients in the vicinity of the critical point [7]. Recently the technique was adapted to study transitions

in polymeric systems under pressure of compressed supercritical fluids (SCF) [16]. The supercritical polymer transitiometry can be very easily adapted to investigation of other types of transitions, such as precipitation or crystallization from a supercritical phase. Scanning transitiometry should also be very helpful in teaching thermodynamics and materials science.

This paper presents selected results of investigations made with three scanning transitiometers which are all high pressure constant mass calorimeters working in isothermal or nonisothermal conditions. This serves to illustrate performances and operating ranges of transitiometry applied to polymer science.

2. MEASUREMENTS

2.1. Materials

The three investigated polyethylenes were: low-density polyethylene, LDPE, (Lotrex FC 1010) crystalynity 0.39; medium-density polyethylene, MDPE, (Finantrene 3802) crystallnity 0.59; and high-density polyethylene, HDPE, (Marlex 56020) crystallinity 0.73, respectively.

Poly(vinylidene fluoride), PDVF, used in the present study was kindly supplied by Total-Fina-Elf and had the following characteristics: M_n=113000 and M_w=330000.

The gases, 1,1-difluoroethylene, CH_2F_2, (+99%, Aldrich Chemical Company, Inc.), nitrogen (SAGA, France), and carbon dioxide (SAGA, France) were used without purification. The critical pressure and temperature for CO_2 and $C_2H_2F_2$ are 7.38 MPa and 31 °C, and 5.82 MPa and 78.3 °C, respectively [17]. Wheat starch powder was from PROLABO, France, catalogue number 21 146 290 with amylose content 21.0±0.2 %, lipid content 0.27±0.01 % and protein content 0.36±0.01 %. In order to prepare a water emulsion or a paste a given amount of demineralised and bidistilled water was added to a weighted sample of starch powder and the mixture was carefully blended manually until a homogeneous phase was obtained. The vulcanised rubber used in this study was a poly(butadiene-*co*-styrene) rubber with T_g of –26 °C at atmospheric pressure (determined with a Metller Toledo DSC 821^e apparatus at 5 Kmin^{-1}).

2.2. Method

The new method presented here uses the basic principles of scanning transitiometry, previously described [13]. For the majority of selected examples the investigated polymer or polymer-based mixture was placed in the high pressure measuring cell surrounded by the sensitive calorimetric detector and a transition or a change in state was induced by a controlled variation of an independent variable (p,V, or T) while the other independent variable was kept constant. In all cases the variations of the dependent variable as well as the associated heat effects were simultaneously recorded as a function of time or of the scanned variable. Results of a transitiometric experiment are always a pair of simultaneous thermodynamic derivatives (thermal and mechanical) or a pair of thermomechanical coefficients [(α_p and κ_T); (γ and κ_T); (C_p and α_p); or (C_V and γ), depending on the selection of the pair of independent variables]. Excepting part of subsection 3.2. dealing with the influence of gas sorption, the reference cell was kept

only as a thermal reference. In almost all cases the polymer sample was in direct contact with the pressure transmitting fluid, the only exception concerns the study of biopolymers gelatinization were the wheat starch/water mixtures were encapsulated into a flexible lead ampoule. For the low temperature investigations the mercury was replaced with *n*-propanol (T_m = -97 °C).

2.3. Instrument

A detailed scheme of the instruments used in this study and constructed according to the principle of scanning transitiometry is presented in Fig. 1.

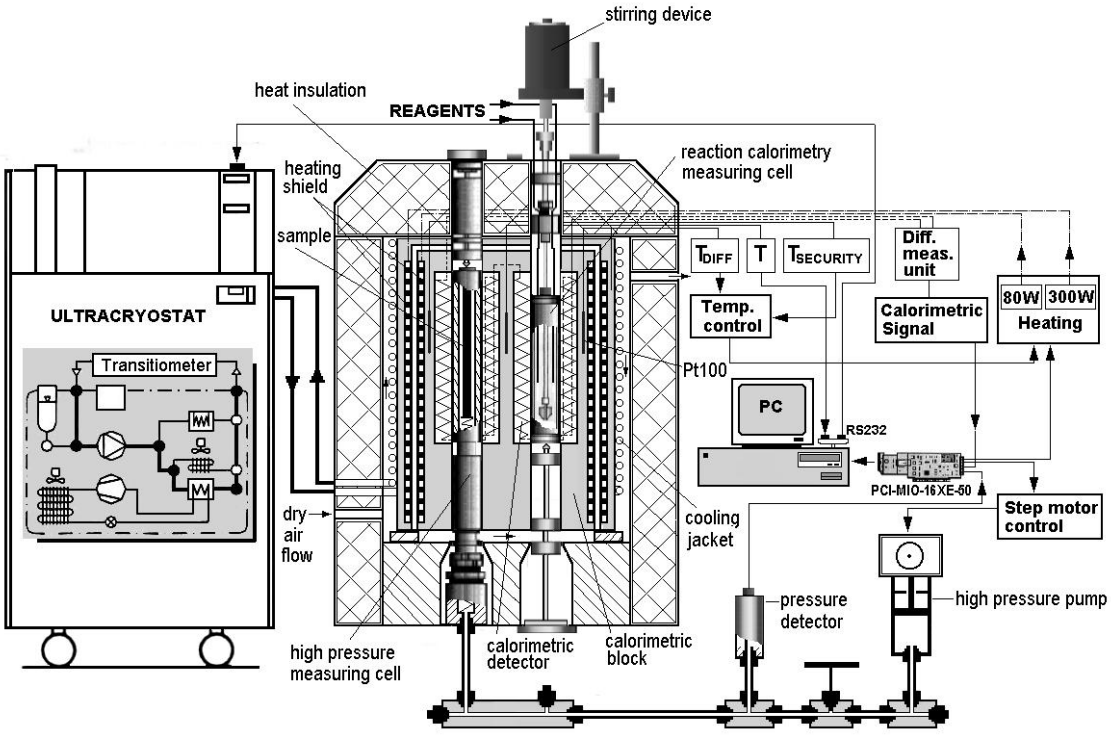

Figure 1. A detailed scheme of a transitiometric installation for simultaneous and *in situ* analysis of thermal and volumetric properties of polymers at pressures up to 200 MPa and over the temperature range from 173 to 570 K. In this Figure, for convenience the two types of cells are shown (on the left-hand side the high-pressure cell and on the right-hand side the reaction cell).

It consists of a calorimeter equipped with high-pressure vessels, a *pVT* system, and a LabVIEW based virtual instrument (VI) software. Two cylindrical calorimetric detectors (Φ=17 mm, l=80 mm) made from 622 thermocouples chromel-alumel each are mounted differentially and connected to a nanovolt amplifier. The calorimetric detectors are placed in a calorimetric metallic block, the temperature of which is directly controlled with an entirely digital feedback loop of 22 bit resolution (~10^{-4} K), being part of the transitiometer software. The calorimetric block is surrounded by a heating-cooling shield. The temperature difference between the block and the heating-cooling shield is set constant (5, 10, 20 or 30 K) and is controlled by an analogue additional controller. The temperature measurements, both absolute and differential, are performed with calibrated Pt 100 sensors. The heaters are homogeneously embedded on the outer

surfaces of both the calorimetric block and the heating-cooling shield. The whole assembly is placed in a thermal insulation enclosed in a stainless steel body and placed on a stand, which permits to move the calorimeter up and down over the calorimetric vessels. When performing measurements near 273 K or below, dry air is pumped through the apparatus. A detailed description of the transitiometer is given elsewhere [18].

3. RESULTS ON SELECTED SYSTEMS

To illustrate performances and advantages of scanning transitiometry in polymer science three main typical applications have been selected: *i*) transitions of polymer systems under various constrains, including first-order phase transition, glass transition and biopolymer gelatinization; *ii*) polymer thermophysical properties and influence of gas sorption; *iii)* polymer particle synthesis.

3.1. Transition of polymer systems under various constrains

Different transitions of polymer systems under various constrains like pressure, temperature and/or chemical reagents are reported hereafter.

First order phase transition

To begin with the simplest case, the first-order phase transition of semicrystalline polymers in the presence of a chemically inert fluid as pressure-transmitting fluid is discussed. Mercury was preferred due to its chemical inertia and very good and well-known thermomechanical coefficients (α_p=1.80×10^{-4} K^{-1} and κ_T=0.40×10^{-4} MPa^{-1}). The polymer sample was always in intimate contact with the pressure transmitting fluid.

In the first example, Fig. 2(a), the pressure effect on the melting/crystallization temperature of MDPE sample is illustrated. The isobaric temperature scans were performed at a rate of 0.833 mKs^{-1}. As it can be seen in Fig. 2(a), both the fusion and crystallization are shifted toward the higher temperatures with the pressure.

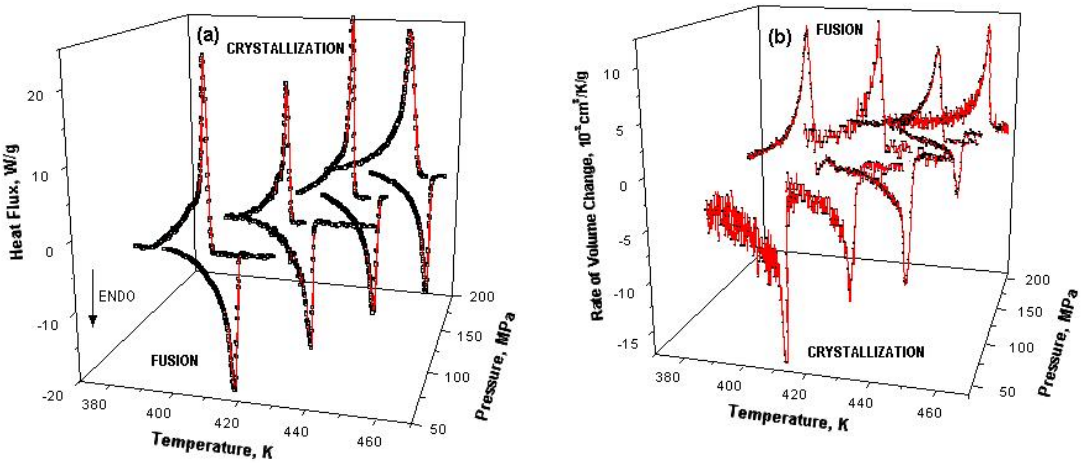

Figure 2. Transitiometric traces obtained simultaneously *in situ* at various pressures for MDPE: (a) heat flux evolution during fusion and crystallization; (b) the rate of volume changes induced by the temperature scan.

Fig. (2b) shows the corresponding rate of volume variations measured simultaneously in the same experiments. Taking as an example, the fusion at 200 MPa, the rates of variations with temperature of both volume and heat gave the same value of the melting temperature, i.e 456.2 K. Variations of volume and of entropy in the same process were obtained by integration of curves from Fig.s 2(a) and 2(b) the corresponding values being of 0.0573 cm^3g^{-1} and -88.54 Jg^{-1}, respectively [6]. The obtained value of 0.297 $K{\cdot}MPa^{-1}$ for $\Delta T_m/\Delta p$ (Clapeyron slope) is in fairly good agreement with the known literature values.

The scanning transitiometric technique was also adapted to work under supercritical conditions. In this case, the pressure transmitting fluid is the gas itself in supercritical state. The polymer sample was contained in an open glass ampoule supported on a spring in the reaction cell (in order to be positioned in the central active part of the detector zone) and in direct contact with the pressurization fluid. The reaction vessel was connected to a pressure gauge and to the pump through a stainless steel high-pressure capillary tube; it can be also connected to a supercritical fluid tank for filling the fluid into the pump.

The systems PVDF/$C_2H_2F_2$ and PVDF/N_2 have been selected to illustrate this particular case. It was proved that $C_2H_2F_2$ dissolves PVDF at high pressure and temperatures, whereas the nitrogen is known as being inert with respect to the polymers and a comparative investigation should be of interest. Fig. 3(a) shows the influence of $C_2H_2F_2$ in the pressure range from 0.1 to 180 MPa on the melting and crystallization of PVDF. One can notice that the fusion peaks span is greater than the corresponding crystallization peaks irrespective of pressure, which is not observed in the case of MDPE [see Fig. 2(a)]. One the other side, with increasing pressure, especially above 40 MPa, the crystallization/fusion peaks broadened largely and continuously while the amplitude of the peaks concomitantly decreases.

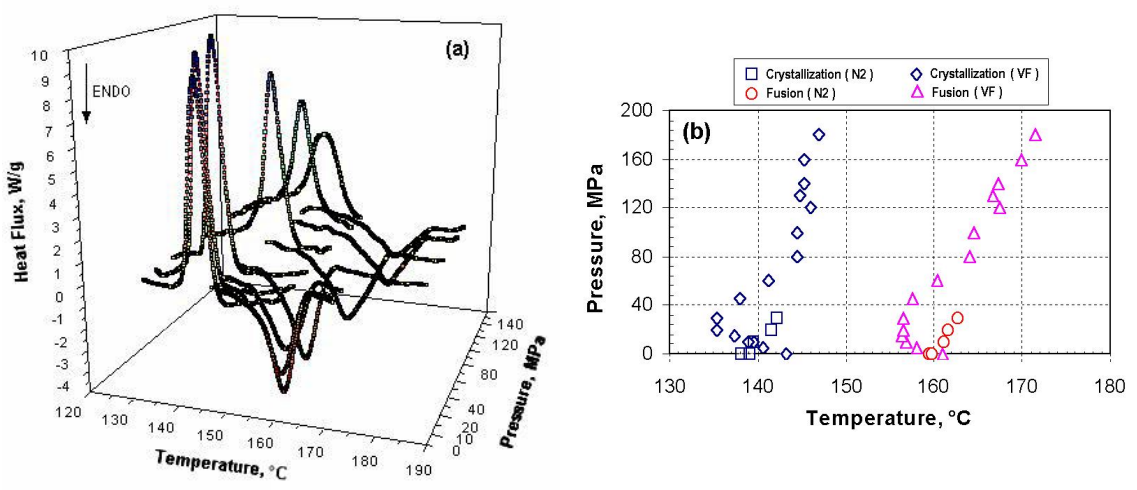

Figure 3. Pressure effect on the temperature-induced and gas-assisted melting/crystallization of PVDF: (a) heat flux evolution during fusion and crystallization in the presence of supercritical $C_2H_2F_2$ (VF); (b) partial *p-T* phase diagram for the PVDF-VF and PVDF-N_2 systems. Note the depression in the melting/crystallization temperature in the pressure range up to 30 MPa for the PVDF-VF system.

Fig. 3(b) shows the influence of $C_2H_2F_2$ as well as of N_2 on the temperatures of melting, T_m, and crystallization, T_{cr}, respectively. Clearly both temperatures increase with increasing the N_2 pressure, similarly to the effect observed with mercury on MDPE in

Fig. 2. In the investigated range of pressure (0.1 to 30 MPa) the slope of T_m-pressure plot and T_{cr}-pressure plots were 0.108 $KMPa^{-1}$ and 0.115 $KMPa^{-1}$, respectively. On the contrary, a $C_2H_2F_2$-assisted melting/crystallization point depression by sorption of gas in polymer up to 30 MPa followed by the antiplasticization effect of the hydrostatic pressure of $C_2H_2F_2$ was found for the PVDF/ $C_2H_2F_2$ system. Consequently, the location of the crystallization and melting boundaries are a compromise between the effect of hydrostatic pressure, which increases the transitions (crystallization and fusion) temperatures, and the solubility of the monomer ($C_2H_2F_2$) in the polymer-rich phase, which depresses these values.

Glass-Transition Temperature

Glass transition temperature is also affected by pressure since an increased pressure causes a decrease in the total volume and an increase in T_g is expected based on the prediction of decreased free volume. This result is important in engineering operations such as molding or extrusions, when operation too close to T_g can result in a stiffening of the material.

Investigation of the glass-transition of polymers under pressure is not a simple problem, especially in the case of elastomers whose T_g are usually well-bellow the ambient temperature. In this case the traditional pressure-transmitting fluid, mercury, must be replaced since its crystallization temperature is relatively high, i.e. about 235.45 K. The choice of the replacement fluid is a challenge because it should be chemically inert with respect of the investigated sample (with respect to all its constituents). Also values of its thermomechanical coefficients, compressibility, κ_T, and thermal expansivity, α_p, which should be smaller than those of investigated samples in *pVT* measurements. An additional difficulty in investigation of second order type transformations is the relatively weak effects measured. It is well-known that the amplitude of T_g increases with the temperature scanning rate while the time-constant of Tian-Calvet type calorimeters imposes typical temperature scan rates which are to slow as compared to current DSC rates. However, with the use of an ultracryostat the temperature of the calorimetric bloc can be well controlled down to 198 K. In addition, for scanning temperature we have used the temperature program illustrated in the insert of Fig. 4(a). This means that the temperature of the cooling liquid is lower than that of the calorimetric bloc during the stabilization period (isothermal segments) and it is higher during the dynamic segment. In such a way, the scanning rate was increased up to 0.7 $Kmin^{-1}$ always keeping a minimal difference between target and real temperatures of the calorimetric bloc. On the other hand, since the temperature gradient between the "heating fluid" and the calorimetric bloc was kept constant (20 K) the power uptake of the heating elements was quasi constant, so the interference of sudden changes of power uptake on the calorimetric signal were avoided. The mere calorimetric response of a poly(butadiene-*co*-styrene) vulcanized rubber during an isobaric scanning of temperature at 50 MPa with temperature ranging form 218.15 K to 278.15 K (0.4 $Kmin^{-1}$) is illustrated on Fig. 4(a).

Fig. 4(b) shows the evolution of T_g at different pressures, at 0.25, 10, 30, 50, and 90 MPa, respectively. As is seen in the insert of this Figure the T_g increases almost linearly with pressure with a slope of 0.193 K/MPa. It should be noted that T_g is expressed as the temperature corresponding to the peak of the first derivative of the heat flux (i.e. the inflexion point of the heat flux).

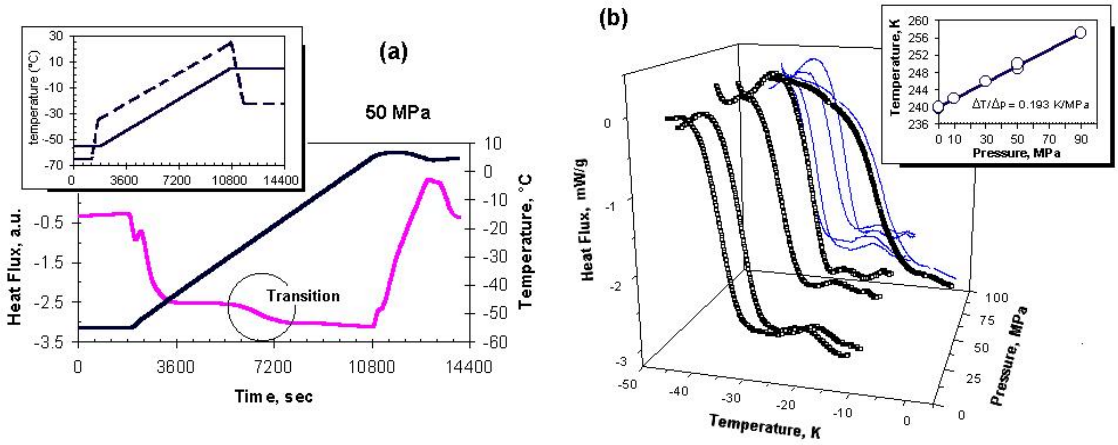

Figure 4. Illustration of scanning transitiometry for low-temperature high-pressure investigation of polymers glass transition: (a) experimental plots obtained during an isobaric temperature scan at 50 MPa (SBR, sample mass = 1.56 g, scanning rate 0.4 $Kmin^{-1}$). In the insert the temperature program for the transitiometer (full line) and heat transfer fluid (dashed line) are depicted; (b) pressure effect on the glass transition temperature, $T_{g,}$. In the insert the pressure coefficient of the glass transition temperature is given.

Biopolymers gelatinization

A fundamental understanding of the influence of processing on food products requires studies, which elucidate how the physical properties of food materials vary as a function of conditions which are encountered in processing. The main processing variables are temperature, pressure and water content. Temperature and water content have already been extensively used as variables in physicochemical investigation of food materials performed with various techniques. However, pressure has been used very seldom, especially when it is concerned with *in situ* studies [19,20]. But there is no doubt that temperature and pressure have an equivalent importance as thermodynamic variables. Apart from the direct relation to the extruder processing conditions, there are several other reasons to measure the effect of pressure on a wide variety of bio-systems important in food science and industry. The most important argument is that one can separate the effects of volume and thermal energy changes, which appear simultaneously in temperature scanning experiments [21]. Molecular processes, which alter the volume of the system, are especially sensitive to pressure. Volume changes associated to biochemical processes can therefore be revealed using pressure as an experimental variable.

The performance of the scanning transitiometry is demonstrated here with a novel *in situ* investigation of pressure effects on the phase transformations occurring during gelatinization of (wheat starch + water) emulsions. In this case the wheat starch/water mixture was placed in a small plastic pouch to separate it from the pressuring fluid. As an example of the advantage of the technique Fig. 5 presents results obtained in isobaric experiments by scanning temperature at a rate of 0.15 $Kmin^{-1}$ at pressures of 10 and 60 MPa, respectively, for a wheat starch - water emulsion at 56 % of water content. Results at each pressure present two output signals recorded simultaneously: the heat flux (rate of heat exchange) and the rate of volume variations as a function of temperature (thermal expansion), both quantities expressed per gram of the investigated emulsion. The most important observation is that all the transitions recorded previously at a temperature scanning rate of 1 $Kmin^{-1}$ with a high sensitivity

classic DSC at atmospheric pressure [22] are also shown by the transitiometric traces in Fig. 5 performed under elevated pressures.

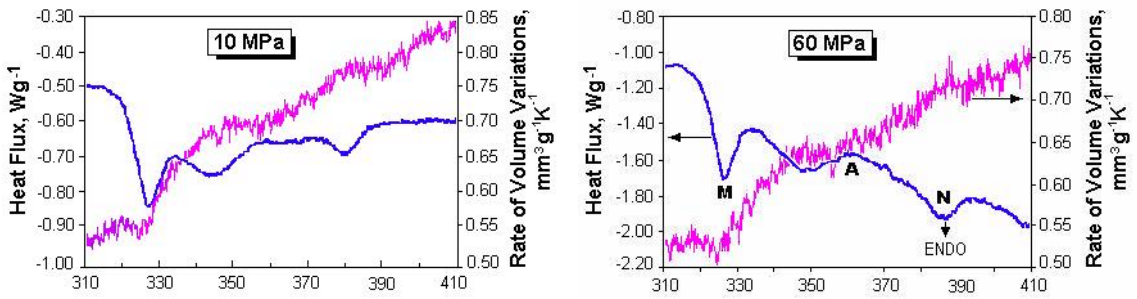

Figure 5. Transitiometric traces obtained simultaneously and *in situ* at 10 and 60 MPa for a starch - water emulsion with 56.0 wt. % water content. Note the volume contraction corresponding to the fusion peak M.

This means that the present technique is a kind of an advanced development of previous classic techniques. As a matter of fact, this novel technique permits to study not only the pressure influence on the course of transitions previously observed at atmospheric pressure, but also to record simultaneously and *in situ* an independent information on the volume variations at those transitions. In this respect one can see on Fig. 5 that the volume variations at the main endothermic transition (***M***) are always negative over the pressure range under investigation. One also can notice that the volume variations at the other particular transitions are rather small, while the general tendency of the volume variations over the whole temperature range is to rise considerably with temperature what can be associated with an important swelling of starch during gelatinization. The main endothermic transition (***M***) is shifted a bit to lower temperatures when pressure is rising what is thermodynamically consistent with the negative volume variation for that transition. Opposite to the main endothermic transition, the pressure influence on both the exothermic transformation (***A***) and the high-temperature small endothermic transition (***N***) is positive. Under pressure of 10 MPa the exothermic transformation starts at (348.6 ± 0.6) K and then is shifted by pressure to higher values at a rate of (38.9 ± 9.9) $mKMPa^{-1}$, while the high-temperature endothermic transition starts at (382.7 ± 0.2) K and then is shifted by pressure to higher values at a rate of (96.1 ± 3.4) $mKMPa^{-1}$.

3.2. Polymer thermophysical properties and influence of gas sorption

Thermal expansion of polymers is a subject of considerable importance to both polymer scientists and engineers. In a first example, the scanning transitiometry has been applied for measuring the isobaric thermal expansivities (α_p) of crystalline polyethylenes as a function of pressure up to 300 MPa at various temperatures. The measurements have been performed for polyethylenes with various degrees of crystallinity, χ_{cr}, at 302.6, 333.0, 362.6, and 393.0. In that case the measurements were based on the Maxwell relation, which states that the isothermal pressure derivative of entropy is equal with opposite sign to the isobaric temperature derivative of volume. Thus, a calorimetric measurement of heat exchanged by a substance submitted to an isothermal pressure change leads to the determination of thermal expansion of the substance under investigation. Mercury was used as an inert hydraulic fluid in which the polymer sample was plunged. A detailed analysis of the working hypothesis and equations to access the

isobaric thermal coefficients as well as the iterative procedure elaborated for derivation of α_p was given elsewhere [10].

Isobaric thermal expansivities of polyethylenes of various densities follow the usual general behavior of pressure and temperature dependence; α_p increases with temperature and decreases with pressure. Fig. 6(a, b, and c) illustrates the pressure effect on the α_p for the three investigated polyethylenes at the above-mentioned temperature range. In all cases, the absolute magnitude of α_p and its strong dependence on both pressure and temperature are observed. As expected, the most sensitive particularly with respect to temperature was LDPE followed by MDPE and finally by HDPE. With pressure increasing, α_p decreases; the decrease is sharper for LDPE. Typically, α_p of polyethylenes of a given density shows the general trend to converge at high pressures.

As an example, in Fig. 6(d) the thermal expansitivities are presented as a function of the degree of crystallinity of polyethylenes at various pressures, at 302.6 K. One can see an almost perfect linear dependency of α_p on the degree of crystallinity. The straight lines in this Figure have been obtained by least squares fitting of experimental data. From such linear approximations α_p of both the amorphous phase (χ_{cr}= 0) and of the crystal phase (χ_{cr}= 1) could be derived. In Fig. 6(e) are presented the thermal expansivities of low-, medium-, and high-density polyethylenes, which compare well with the estimated thermal expansivities of the amorphous and crystal polyethylene phases as a function of pressure up to 300 MPa at 302.6, 333.0, and 363.0 K. At 302.6 K and 0.1 MPa the exact value of α_p for the crystal phase is 2.81×10^{-4} K^{-1}; the corresponding literature value is 2.85×10^{-4} K^{-1} [23]. Similar agreement was also observed between the present data for the crystal phase at atmospheric pressure at 333.0 K and the values calculated from the theoretical equation of state of Pastine for polyethylene [24,25]. Similarly, at 302.6 K and at atmospheric pressure the agreement is also within a few percent [see Fig.6(f)].

The second part of this subsection is devoted to the interactions between semicrystalline polymers, MDPE and PVDF, and two fluids one chemically active, CO_2, and one inert, N_2, at temperatures between T_g and T_m. Basically, taking into account the differential principle of the instrument, two methods have been employed to investigate the interactions. In the first method the polymer sample is placed in the measuring cell where it is in contact with the fluid. The reference cell acts as a thermal reference and an additional blank experiment (under identical conditions) is performed when replacing the polymer sample by an inert material of similar volume (i.e. metal, ceramic, and/or glass). The subtraction of the heat effects recorded from the blank experiment allows to quantify the thermal effect of polymer-fluid interaction. In the second method, employed here for the first time, one experiment is performed in which the polymer sample is placed in the measuring cell while an inert sample of equal volume seats in the reference cell, both cells being connected to the pressure line. Under the assumption that the internal volumes of the of the two cells mounted differentially are exactly equal, during the fluid injection the energy developed inside the cells should also be exactly equal, but of opposite signs and thus they should compensate completely. The measured calorimetric signal is in this case proportional to the thermal effect due to the polymer/fluid interactions.

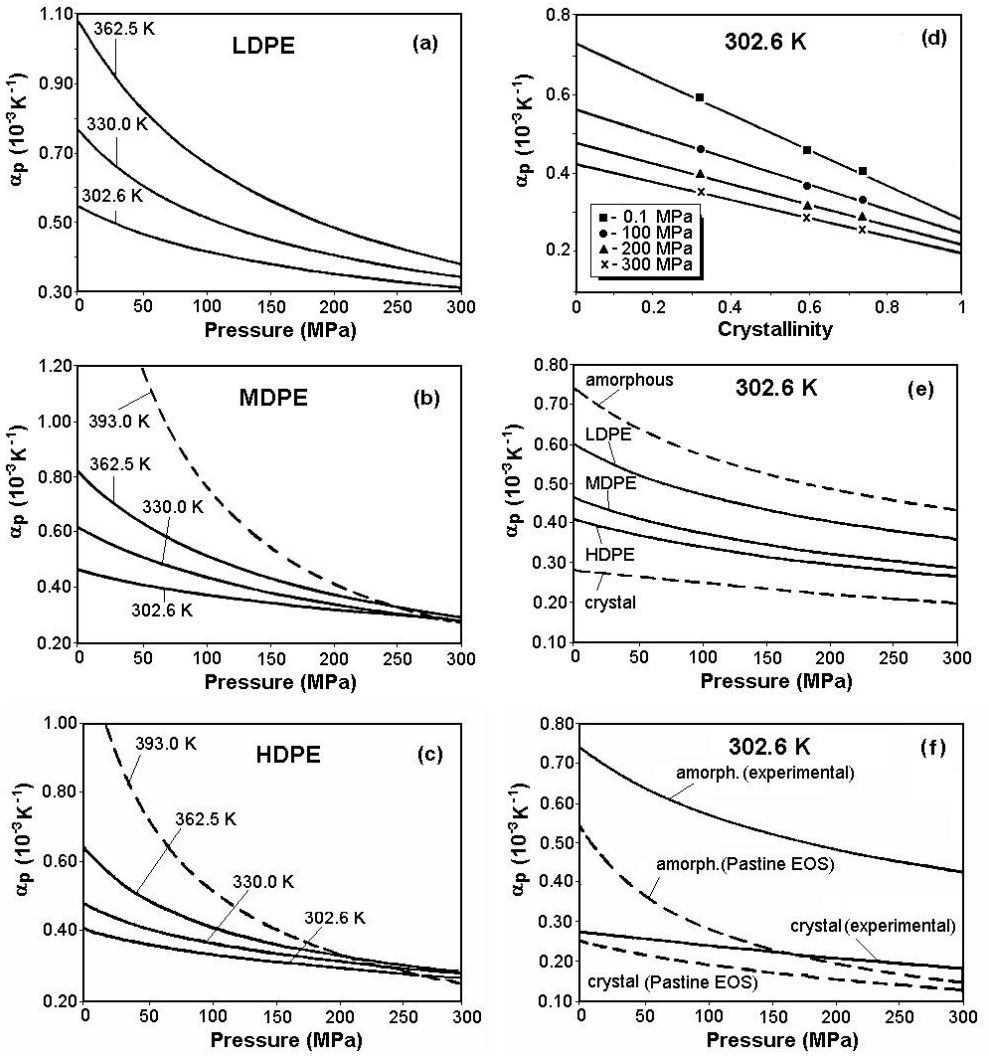

Figure 6. Transitiometric investigation of the pressure effect on the isobaric thermal expansivities of various polyethylenes with different degrees of crystallinity. Effect of temperature on: (a) LDPE; (b) MDPE; and (c) HDPE. Extrapolation of the experimental data to the pure crystalline and amorphous phases at 302.6 K: (d) evolution of α_p with the crystallinity (points represent the experimental data and the lines were obtained by least squares fitting of data); (e) comparison between the experimental α_p and the predicted values for crystal and amorphous phases obtained by approximation from linear fitting of the experimental data; (f) α_p for amorphous and crystal phases of polyethylene obtained using scanning transitiometry and calculated from the Pastine theoretical equation.

Fig. 7(a) shows some selected calorimetric responses for each of the two polymers at constant temperature (353.15 K) and under fast pressure changes. The pressure was step-wise varied in the range from 0.1 to 100 MPa with pressure jumps varying between 6 and 28 MPa. Despite of high compression in each step the differential measured heat flux was very small, few $mWcm^{-3}$ of polymer, which proves the correct thermal balance of the set-up.

For both polymers the measured effects were exothermic, passing through a minimum in the pressure range from 10 to about 30 MPa. At low pressures, up to 20 MPa, the thermal heat flux is greater for the PVDF/CO_2 system. The base line is achieved after about 1hr in this range of pressure. Above 20 MPa the heat of interaction for MDPE/CO_2 overpasses the heat for PVDF/CO_2 system. However, the recorded heats

become eventually identical at high pressures. Above 20 MPa the base line is faster reached, usually in less than 30 min. Remarkably, with nitrogen - a relatively inert fluid - the heat effects slightly increase with pressure for both MDPE and PVDF.

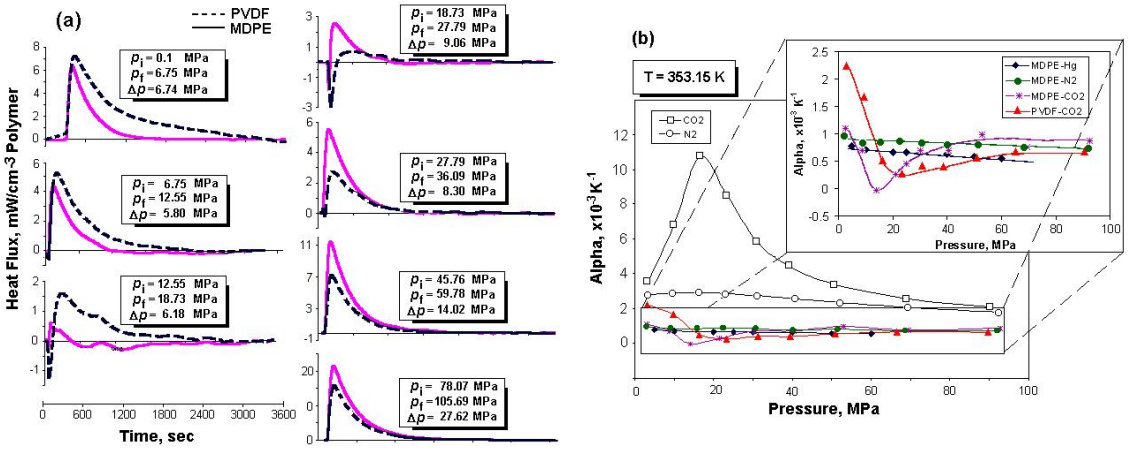

Figure 7. High-pressure scanning transitiometry and gas sorption influence on the polymers thermophysical properties: (a) selected experimental plots of the recorded heat flux during the pressure jumps in the range from 0.1 to 100 MPa. Note that up to 20 MPa the enthalpy of interactions for PVDF-CO_2 system is higher than those corresponding to the MDPE-CO_2 system; above this pressure the interactions MDPE-CO_2 prevails over PVDF-CO_2 ones; (b) comparison between the isothermal expansivities of the pure fluids (CO_2 and N_2) and of Hg-, N_2-, and CO_2-presseurized MDPE and PVDF.

Under the assumption that there are no interactions between the metal rod and the fluid, and making use of Maxwell equation one can get the isobaric thermal expansivities (α_p) of the saturated polymers at a given pressure. Fig. 7(b) illustrates the comparative evolution of α_p in presence of different fluids, *i.e.* mercury-pressurized MDPE, N_2-pressurized MDPE, CO_2-pressurized MDPE and CO_2-pressurized PVDF, respectively. Strikingly, in the case of CO_2, where α_p of the fluid is about one order of magnitude higher with a maximum around 20 MPa, α_p of the saturated polymer (MDPE or PVDF) exhibits mirror-image minimum at almost the same pressure. In the case of Hg-pressurized and N_2-pressurized polymers α_p shows a tendency to decrease with pressure, more marked in the case of Hg-pressurized MDPE. In addition, α_p remains always higher in the case of N_2-pressurized MDPE.

3.3. Polymer Particle Synthesis

In the case of polymer synthesis, the scanning transitiometer can be used as a reaction calorimeter, the advancement of a polymerization reaction being accurately monitored through the rigorous control of the thermodynamic parameters. The differential configuration allows to eliminate most of the systematic errors related to the experiment and/or heat transfer. The small thermal resistance makes it possible to work in a quasi-isothermal regime without power compensation, which is another major advantage of the present configuration. Results obtained from such measurement are to a large extent independent of the wetted surface or the stability of heat transfer, so that viscosity, minor changes in stirrer speed or evaporation do not have to be taken into account here.

To gather additional information on a reaction we developed a reaction cell which combines *in situ* UV/Vis/NIR spectroscopy making use of a small optical probe

coupled to a miniaturized spectrometer. In addition, the cell accommodates a stirrer and injection capillaries allowing different dosing profiles for one or two reactants.

The performances of this instrument are illustrated in the case of a processes for which reaction calorimetry was up to now difficult to apply, such as precipitant polymerization, particularly the ultrafine polyamide (PA) particles synthesis by anionic polymerization of lactams in aprotic solvents. Anionic polymerization of lactams in organic solvents is a complex process, the most important steps in granularly or powdery polyamide formation are the following ones: initiation and growth of macromolecules in homogeneous medium, nucleation, phase separation and aggregation of the growing chains, solidification and, finally, polymer crystallization. All above-mentioned events occur rapidly and partially overlap [26].

The polymerization occurs by the activated monomer mechanism, which supposes a two-step propagation mechanism involving the acylation of the lactam anion (NaL) by the *N*-acyllactam end-group of the growing chain followed by a fast proton-exchange with the monomer.The net result of each propagation step is the incorporation of a monomer unit into the polymer chain and the regeneration of the two active species [27].

In order to avoid the slow initiation step, the preformed *N*-acyllactams or their precursors (so called chain initiators, C.I.) are introduced in the system:

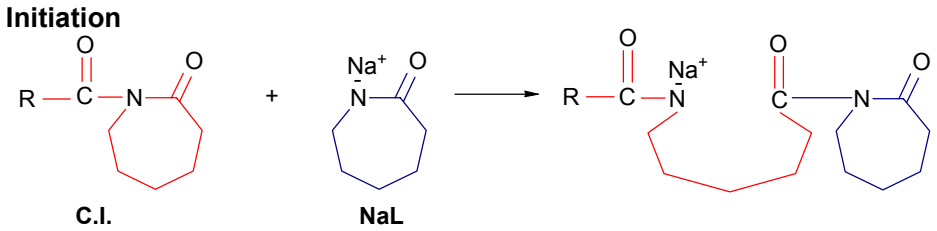

In the very strong basic medium the C.I. goes rapidly in side-reactions (Claisen condensation) and the polymerization is prematurely stopped [28]. Consequently, as long as the monomer remains in the reaction medium the polymerization can be continued simply adding a new amount of chain initiation. In other words, the polymerization can be stopped and restarted by controlling the amount of C.I.

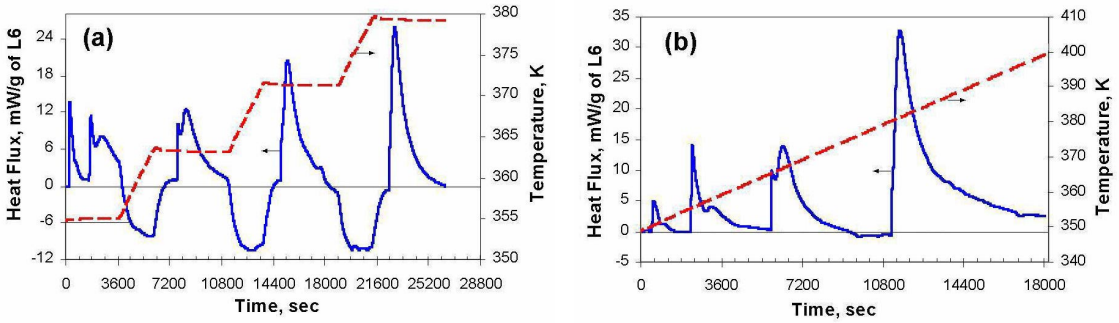

Figure 8. Illustration of the temperature effect on the evolution of the heat released during anionic polymerization of caprolactam: (a) isothermal measurements at four temperatures (355, 363, 371, and 379 K, respectively); (b) non-isothermal measurements during four injections of C.I. (temperature scan between 353 and 398 K at 0.12 $Kmin^{-1}$).

A detailed analysis of the strong temperature influence, has been possible through the measured heat flux under isothermal - at four successive temperatures, Fig. 8(a) - or nonisothermal conditions - temperature scanning, Fig. 8(b). Clearly, the shape

of the curves representing the heat evolution with polymerization, passes from two peaks at low temperatures (up to 363 K) to a large shoulder [clearly seen in Fig. 9(b)] that diminishes around 375 K, and finally disappears at high temperature (above 393 K). The intensity of the first peak is not influenced by temperature but the intensity of the second one strongly increases with temperature, and consequently the monomer conversion increases too.

Using *in situ* Vis spectroscopy (see Fig. 9) it was established that the first peak corresponds to the initiation reaction, i.e. between the two catalytic species (a very fast reaction), while the second one is composed by the thermal contribution of the propagation reaction and of polymer crystallization during the phase separation. Under nonisothermal conditions (temperature scanning) the same trend of heat evolution was observed, Fig. 8(b). A 3D representation of the spectrometric signal evolution versus time at 363 K is given in Fig. 9(a). It is worth noting the stability of intensity in the homogenous medium and its sharp decrease right upon the beginning of phase separation (polymer precipitation). The combination of the two signals, Fig. 9(b), clearly demonstrates that the second peak arises almost at the same time as the phase separation.

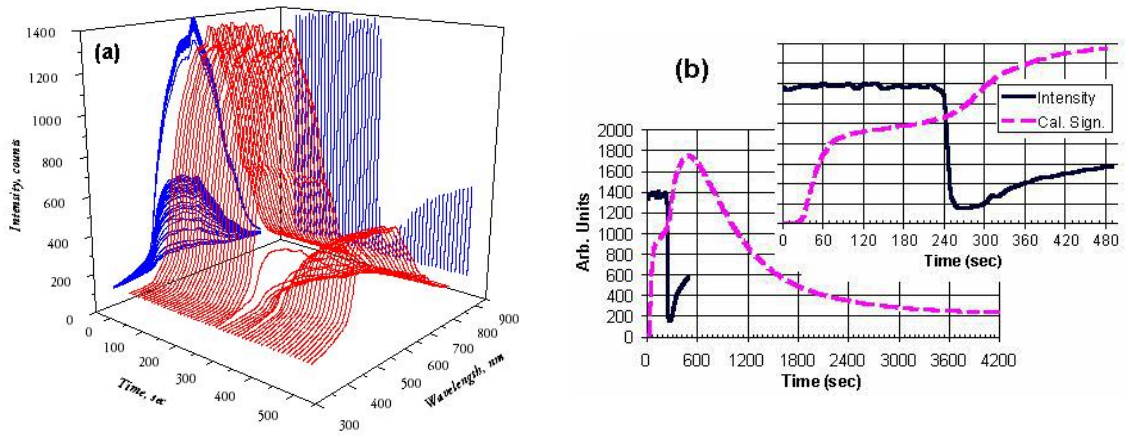

Figure 9. Online combination of calorimetry and spectroscopy: (a) 3D plots of the evolution of spectrometric signal during the anionic polymerization of caprolactam; (b) simultaneous calorimetric and spectroscopic signals recorded during polymerization at 363 K (the intensity of spectrometric signal was taken at 600 nm). Note the stability of the spectroscopic signal before the phase separation and its sharp decrease at phase separation.

The main advantage of this process is related to the possibility of orienting it toward the preparation of powders with desired morphologies through a fine tuning of the synthesis parameters. To this goal it was demonstrated that one of the most convenient modality is to continuously deliver the amount of C.I. over a long period Fig. 10(a) [29]. In the case of continuous adding of C.I. three important indications are provided by the spectroscopic data, Fig. 10(b). The first one [I in Fig. 10(b)] concerns the period between the start of reaction and the beginning of polymer precipitation; it depends on temperature and on injection rate of C.I.. The second one [II in Fig. 10(b)] is related to the particle size evolution with time (this is only a qualitative information). Generally, after the phase separation the evolution of spectroscopic signal runs parallel to the conversion. As is seen in Fig. 10(b) when one approaches the end of process the intensity of spectrometric signal remains constant. Finally, the third information (also qualitative) refers to the average size of particles. It was proved by SEM [see inserts of

Fig. 10(b)] that the average particle size is directly proportional to the final intensity of spectrometric signal [III in Fig. 10(b)].

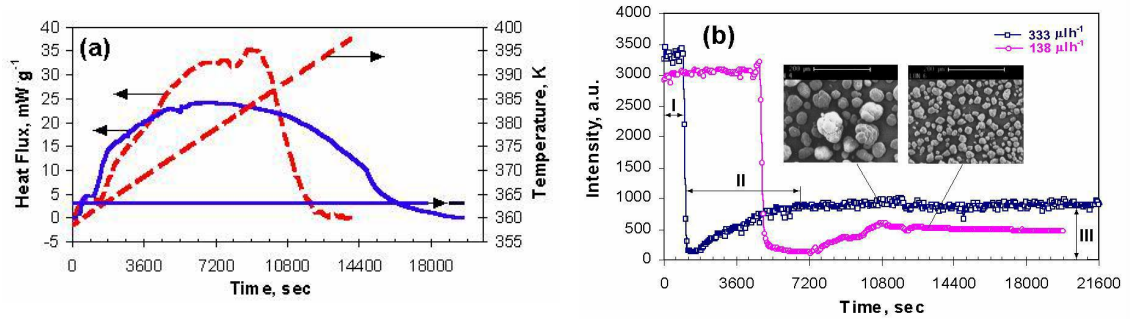

Figure 10. Illustration of reaction calorimetry as a tool for process optimization: (a) controlled evolution of the heat flux by continuous adding of C.I. over a preestabished period, here 4h with a rate of 60 μLh^{-1} under isothermal (full lines) and non-isothermal conditions(dashed lines); (b) online qualitative development of particles and of their final size based on evolution of the intensity of spectrometric signal for different rates of feeding of C.I., i.e. 138 and 333 μLh^{-1}, respectively. The reaction temperature was 378 K and the intensity of spectrometric signal was recorded at λ = 600 nm. In the inserts, the corresponding SEM micrographies of the obtained particles are given.

References

1. L. H. Sperling, *Introduction to Physical Polymer Science,* 3rd Ed., (Wiley, New-York, 2001), p. xxix.
2. S.L. Randzio, *Thermochim. Acta* **355**:107 (2000).
3. P. Rollet and R. Bouaziz, *L'analyse thermique,* Vol. *Tome 1: Les changements de phase,* (Gautier-Villars, Paris, 1972) p. 3577.
4. G. W. H. Höhne, *Thermochim. Acta* **332**:115 (1999).
5. Z. Zhang and Y. P. Handa, *Macromolecules* **30**:8505 (1997).
6. S. L. Randzio, *J. Therm. Anal. Cal.* **57**:165 (1999).
7. S. L. Randzio, J-P. E. Grolier, and J. R. Quint, *High Temp.-High Pressures* **30**:645 (1998).
8. P. Pruzan, L. TerMinassian, and A. Soulard, *High-Pressure Science and Technology* **1**:368 (1979).
9. S. L. Randzio and J-P. E. Grolier, *Rev. Sci. Instrum.* **65**:960 (1994).
10. Rodier-Renaud, S. L. Randzio, J-P. E. Grolier, and J. R. Quint, *J. Polym. Sci. Part B: Polym. Phys.* **34**:1229 (1996).
11. S.L. Randzio, *Pure Appl. Chem.* **63**:1409 (1991).
12. P. Ehrenfest, *Proc. Kon. Akad. Wetensch.* **36**:153 (1933).
13. S.L. Randzio, *Chem. Soc. Rev.* **25**:383 (1996).
14. S.L. Randzio, *Thermochim. Acta* **300**:29 (1997).
15. S.L. Randzio, *J. Therm. Anal.* **48**:573 (1997).
16. S.L. Randzio and J.-P.E. Grolier, A*nal. Chem.* **70**: 2327 (1998).
17. M. Loro, J. S. Lim, and M. A. McHugh, *J. Phys. Chem. B* **103**:2818 (1999).
18. S.L. Randzio, Ch. Stachowiak, and J-P. E. Grolier, *J. Chem. Thermodynamics* **35**:639 (2003).
19. P. Rubens, J. Snauwaert, K. Heremans, R. Stute, *Carbohydtrate Polym.*, **39**:231 (1999).

20. P. Rubens, K. Heremans, *Biopolymers*, **54**:524 (2000).
21. G. Weber, H.D. Drickamer, *Q. Rev. Biophys.*, **16**:89 (1983).
22. S. L. Randzio, I. Flis-Kabulska,. J-P. E Grolier,. *Macromolecules* **35**:8852 (2002).
23. M. Shen, W. N. Hansen, and P. C. Romo, *J. Chem.Phys.,* **51**:425 (1969).
24. D. J. Pastine, *J. Appl. Phys.,* **41**:5085 (1970).
25. D. J. Pastine, *J. Chem. Phys.,* **49:**3012 (1968).
26. F. Dan and C. Vasiliu-Oprea, *Colloid Polym. Sci.* **276**:483 (1998).
27. H. Sekiguchi, in *Ring-Opening Polymerization,* Vol 2, K. J. Iving and T. Saegusa, eds. (Elsevier, London, 1984), p. 833.
28. J. Stehlicek and J. Sebenda, *Eur. Polym. J.* **22**:769 (1986).
29. F. Dan, J-P. E. Grolier, *Setaram News* **7**:i3,i4 (2002).